

CHALMERS

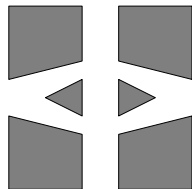
FINITE ELEMENT CENTER



PREPRINT 2004–10

A Posteriori Error Analysis of Stabilized Finite Element Approximations of the Helmholtz Equation on Unstructured Grids

Mats G. Larson and Axel Målqvist



Chalmers Finite Element Center

CHALMERS UNIVERSITY OF TECHNOLOGY

Göteborg Sweden 2004

CHALMERS FINITE ELEMENT CENTER

Preprint 2004–10

A Posteriori Error Analysis of Stabilized Finite Element Approximations of the Helmholtz Equation on Unstructured Grids

Mats G. Larson and Axel Målqvist



CHALMERS

Chalmers Finite Element Center
Chalmers University of Technology
SE-412 96 Göteborg Sweden
Göteborg, April 2004

A Posteriori Error Analysis of Stabilized Finite Element Approximations of the Helmholtz Equation on Unstructured Grids

Mats G. Larson and Axel Målqvist

NO 2004–10

ISSN 1404–4382

Chalmers Finite Element Center
Chalmers University of Technology
SE–412 96 Göteborg
Sweden

Telephone: +46 (0)31 772 1000

Fax: +46 (0)31 772 3595

www.phi.chalmers.se

Printed in Sweden
Chalmers University of Technology
Göteborg, Sweden 2004

A Posteriori Error Analysis of Stabilized Finite Element Approximations of the Helmholtz Equation on Unstructured Grids

Mats G. Larson * Axel Målqvist †

April 8, 2004

Abstract

In this paper we study the Galerkin least-squares method for minimizing pollution when solving Helmholtz equation. We especially consider how stochastic perturbations on a structured mesh affects the optimal choice of the method parameter τ . The analysis is based on an error representation formula derived by a posteriori error estimates using duality. The primary goal with this work is not to present a brand new method for this problem but to show how existing methods derived for structured meshes can be modified to work on unstructured grids. We conclude that a parameter optimized for a structured mesh needs to be increased by a term proportional to the variance of the perturbation to be unbiased on a perturbed grid. We present numerical examples in one and two dimensions to confirm our theoretical results.

1 Introduction

It is well known that the standard Galerkin finite element method suffers from a substantial loss of accuracy when solving the Helmholtz equation for higher wave numbers. The problem is basically that the waves propagate too slow when using the standard Galerkin method. The solution is to increase the numerical wave number.

Previous work. The choice of numerical wave number have been solved by dispersion analysis in one and two dimension. In one dimension it is actually possible to achieve nodal exactness by the Galerkin Least-Squares (GLS) method, see [6, 9, 5], or the Generalized Finite Element Method (GFEM), see [2], and in two dimensions these methods

*Corresponding author, Department of Computational Mathematics, Chalmers University of Technology, Göteborg, S-412 96, Sweden, mgl@math.chalmers.se

†Department Computational Mathematics, Chalmers University of Technology, Göteborg, S-412 96, Sweden, axel@math.chalmers.se

gives significant improvement compared to the standard Galerkin method. The expression "pollution" is often used to describe this phenomenon and it was first stated in [2]. A drawback of using these methods to determine the numerical wave number in higher dimensions is that they are designed to be optimal for one certain direction on a structured grid.

Recent work on variational multiscale methods and subgrid modelling [8, 7] has given an understanding of the origin of GLS. It also represents an alternative to the dispersion analysis that works independent of the structure of the mesh. In a paper dealing with edge elements for electro-magnetic modelling [10] an improvement in accuracy when solving the vector Helmholtz equation was discovered on unstructured grids. This effect can also be seen in numerical studies for example in [5]. These results encouraged us to further investigate this area.

New contributions. Our goal with this paper is to understand how methods for minimizing pollution on structured grids needs to be modified to suit unstructured grids. To create the unstructured grid we start with a structured grid and add perturbations to the nodes from a given distribution. We need a method for computing an optimal method parameter τ on a given mesh. We achieve this by deriving an error representation formula using a posteriori error estimation techniques iteratively and choosing τ so this error functional equals zero. This method is independent of the structure of the mesh and converges to an optimal τ in the sense that a given linear functional of the error is zero for this choice of τ .

We then study a family of meshes with stochastic perturbations δ_i , in each interior node i , and calculate the expected value of τ , $E[\tau]$. In one dimension we get the following result:

$$E[\tau] = Ch^2k^2(1 + 6\text{Var}(\delta_i)), \quad (1.1)$$

where $C < 0$ is a constant that can be calibrated by a standard method on a structured grid e.g. see [5]. This means that the numerical wave number k_h modifies in the following way, $k_h^2 = k^2(1 - \tau k^2)$. From equation (1.1) we see clearly that the average of τ calculated on perturbed grids will not be equal to τ calculated on the structural grid. However we also see that for small perturbations, τ from the structural calculation is a good estimate. The challenge is to extend this analysis to two dimensions where it is much harder to find an optimal τ .

In two dimensions we again derive an optimal τ independent of the structure of the mesh by using an error representation formula based on an a posteriori error estimate. The procedure needs to be done in an iterative fashion. A typical linear functional of the error we study could be an integral over the error over an outflow boundary. Again we recognize a modification of τ proportional to the variance of the perturbation. For a plane wave in two dimensions numerical calculations shows improved results compared to a plane wave in one dimension. We argue that this effect arises from the fact that the variance of on integral of the error on the outflow boundary is smaller than the variance of the error measured in one point. This could explain the effect in [10].

Of course there are numerous advantages of using randomized unstructured meshes

instead of structured ones. When it comes to wave propagation on of the most important are that a randomized mesh is isotropic i.e. "looks the same" in all directions. This means that if we can find an optimal τ for one direction it will work well for waves propagating in an arbitrary direction.

Outline In §2 we present a one dimensional model problem, derive an a posteriori error estimate and state a formula for choosing the method parameter τ . We then study how this choice of τ depends on the structure of the mesh. In §3 we present numerical results for this problem and in §4 we turn our attention to a two dimensional model problem. Again we derive an a posteriori error estimate from which we can calculate the parameter τ . In §5 we present numerical results for two test examples and finally in §6 we draw some conclusions of this work.

2 One Dimensional Model Problem

We consider the following one dimensional model problem: find u such that

$$\begin{cases} -u'' - k^2 u = 0 & \text{in } \Omega, \\ u'(0) = ik, \\ u'(\pi) = ik u(\pi), \end{cases} \quad (2.1)$$

where $\Omega = [0, \pi]$. This setting makes the wave propagate freely from left to right with analytic solution $u(x) = e^{ikx}$. The corresponding weak formulation reads: find $u \in H^1(\Omega)$ such that

$$(u', v') - k^2 (u, v) - ik u(\pi)v(\pi)^* = -ik v(0)^*, \quad \text{for all } v \in H^1(\Omega), \quad (2.2)$$

where (\cdot, \cdot) is the ordinary $L^2(\Omega)$ scalar product and $v(x)^*$ is the complex conjugate of $v(x)$.

2.1 The Galerkin Least-Squares Method

The GLS stabilization, see [6], of the weak form reads: find $u \in H^1(\Omega)$ such that

$$(u', v') - k^2 (u, v) + (\tau Lu, Lv)_{\tilde{\Omega}} - ik u(\pi)v(\pi)^* = -ik v(0)^*, \quad \text{for all } v \in H^1(\Omega), \quad (2.3)$$

where τ is a complex number, $L = -\frac{\partial^2}{\partial x^2} - k^2$, and $\tilde{\Omega}$ is the union of element interiors. This method can now be discretized and we can introduce $p = 1 - \tau k^2$ as the new parameter. If we for the sake of simplicity only consider the space V of piecewise linear base functions we get: find $U \in V$ such that

$$(U', v') - k^2 p (U, v) - ik U(\pi)v(\pi)^* = -ik v(0)^*, \quad \text{for all } v \in V. \quad (2.4)$$

Here we see that the stabilization is done basically by changing the wave number in the Galerkin method, see [6]. Next we present an a posteriori error analysis for the piecewise linear case.

2.2 Error Representation Formula

We would like to choose p in order to minimize a given linear functional of the error $e = u - U$ i.e. (e, ψ) , where ψ is a given function in $H^{-1}(\Omega)$. We begin the a posteriori analysis by presenting the dual problem: find ϕ such that

$$\begin{cases} -\phi'' - k^2 \phi = \psi & \text{in } \Omega, \\ \phi'(0) = 0, \\ \phi'(\pi) = -ik \phi(\pi), \end{cases} \quad (2.5)$$

We proceed with the following calculation,

$$(e, \psi) = (e, -\phi'' - k^2 \phi) \quad (2.6)$$

$$= (e', \phi') - (k^2 e, \phi) - [e\phi'^*]_0^\pi \quad (2.7)$$

$$= -(U', \phi') + (k^2 U, \phi) + [u' \phi'^*]_0^\pi - ik e(\pi)\phi(\pi)^* \quad (2.8)$$

$$= (U'', \phi - \pi\phi) + (k^2 U, \phi - \pi\phi) - (U', \pi\phi) \quad (2.9)$$

$$+ (k^2 U, \pi\phi) + ik U(\pi)\phi(\pi)^* - ik \phi(0)^*$$

$$= (U'', \phi - \pi\phi) + (k^2 U, \phi - \pi\phi) + (\tau k^4 U, \pi\phi) \quad (2.10)$$

$$= (k^2 U, \phi - \pi\phi) + (\tau k^4 U, \pi\phi). \quad (2.11)$$

This calculation suggests that $\tau = -\frac{(k^2 U, \phi - \pi\phi)}{(k^4 U, \pi\phi)}$ or in terms of p ,

$$\boxed{p = 1 - \tau k^2 = \frac{(U, \phi)}{(U, \pi\phi)}} \quad (2.12)$$

would make (e, ψ) small.

Remark 2.1 We also note that if there exists a $\hat{\tau}$ such that $(e, \psi) = 0$ it can always be written on the form $\hat{\tau} = -\frac{(k^2 U, \phi - \pi\phi)}{(k^4 U, \pi\phi)}$ or $\hat{p} = \frac{(U, \phi)}{(U, \pi\phi)}$.

Remark 2.2 In practice ϕ will not be known so we have to calculate it numerically. Since we need to subtract the interpolant we use higher order elements for the dual problem. However this is a computationally expensive way of getting high accuracy and should primarily be used if error control is essential.

It is possible to proceed iteratively starting with $p_0 = 1$ solving equation (2.4) for U_n and choosing,

$$p_{n+1} = \frac{(U_n, \phi)}{(U_n, \pi\phi)} \quad \text{for } n = 0, 1, \dots \quad (2.13)$$

In section 3 we present numerical results that shows fast convergence for this particular algorithm for nodal error control. We are going to use the iterative algorithm described in equation (2.13) to calculate optimal values of p on perturbed grids. In this way we can study how an optimal p depends on the size of the perturbation δ .

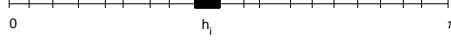


Figure 1: One dimensional unstructured mesh with $n = 19$ and $\delta = 0.4$.

2.3 Unstructured Mesh

We introduce a new parameter $0 \leq \delta < 1$ which is a measure of how unstructured the mesh is. We divide $[0, \pi]$ into n subintervals in the following way,

$$\begin{cases} x_0 &= 0 \\ x_i &= \frac{i\pi}{n} + \delta_i, \quad \text{for } i = 1, \dots, n-1, \\ x_n &= \pi, \end{cases}$$

where $\delta_i \in U([- \frac{\delta\pi}{2n}, \frac{\delta\pi}{2n}])$, see Figure 1. From this definition we note that the interval length $h_i = x_i - x_{i-1}$ the perturbed mesh is equal to $h + \delta_i - \delta_{i-1}$. With this notation we need to define $\delta_0 = \delta_n = 0$. We are interested in how the expected value and the variance of the error (e, ψ) depends on δ , $h = \pi/n$, and k . We now see p as a stochastic parameter \hat{p} and use equation (2.11) to get,

$$(e, \psi) = k^2(U, \phi - \pi\phi) - k^2(\hat{p} - 1)(U, \pi\phi). \quad (2.14)$$

Our aim is to find $p = E[\hat{p}]$ such that $E[(e, \psi)] = 0$ for a given δ . We start with the following Lemma.

Lemma 2.1 *Let $z \in C^2([0, h])$ such that $z(0) = z(h) = 0$, $\varphi_0 = 1 - \frac{x}{h}$, and $\varphi_1 = \frac{x}{h}$. Then we have,*

$$\begin{aligned} \int_0^h \varphi_0 z dx &= -\frac{h^2}{3} \int_0^h \varphi_0^2 \varphi_1 z'' dx - \frac{h^2}{6} \int_0^h \varphi_0 \varphi_1^2 z'' dx, \\ \int_0^h \varphi_1 z dx &= -\frac{h^2}{6} \int_0^h \varphi_0^2 \varphi_1 z'' dx - \frac{h^2}{3} \int_0^h \varphi_0 \varphi_1^2 z'' dx. \end{aligned} \quad (2.15)$$

Proof. We start with $\int_0^h \varphi_i z dx$ for $i = 0, 1$ and integrate by part. We use the fact that $(-h\varphi_0)' = 1$, $(h\varphi_1)' = 1$ and that the boundary term will vanish since $z(0) = z(h) = 0$ to get,

$$\begin{aligned} \int_0^h \varphi_0 z dx &= \frac{h}{2} \int_0^h \varphi_0^2 z' dx, \\ \int_0^h \varphi_1 z dx &= -\frac{h}{2} \int_1^h \varphi_1^2 z' dx. \end{aligned} \quad (2.16)$$

Next we proceed with the first equation in (2.16) and use that $(h\varphi_1)' = 1$ and integrate by parts,

$$\int_0^h \varphi_0^2 z' dx = -h \int_0^h \varphi_1 (\varphi_0^2 z')' dx = 2 \int_0^h \varphi_0 \varphi_1 z' dx - h \int_0^h \varphi_1 \varphi_0^2 z'' dx. \quad (2.17)$$

Since $\varphi_0 + \varphi_1 = 1$ on $[0, h]$ we have,

$$0 = \int_0^h (\varphi_0 + \varphi_1)^2 z' dx = \int_0^h (\varphi_0^2 + 2\varphi_0 \varphi_1 + \varphi_1^2) z' dx, \quad (2.18)$$

inserted in equation (2.17) this yields

$$\int_0^h \varphi_0^2 z' dx = -\frac{1}{2} \int_0^h \varphi_1^2 z' dx - \frac{h}{2} \int_0^h \varphi_0^2 \varphi_1 z'' dx. \quad (2.19)$$

A similar calculation gives

$$\int_0^h \varphi_1^2 z' dx = -\frac{1}{2} \int_0^h \varphi_0^2 z' dx - \frac{h}{2} \int_0^h \varphi_0 \varphi_1^2 z'' dx. \quad (2.20)$$

Together equation (2.19) and equation (2.20) now gives

$$\begin{aligned} \int_0^h \varphi_0^2 z' dx &= -\frac{2h}{3} \int_0^h \varphi_0^2 \varphi_1 z'' dx - \frac{h}{3} \int_0^h \varphi_0 \varphi_1^2 z'' dx, \\ \int_0^h \varphi_1^2 z' dx &= \frac{h}{3} \int_0^h \varphi_0^2 \varphi_1 z'' dx + \frac{2h}{3} \int_0^h \varphi_0 \varphi_1^2 z'' dx. \end{aligned} \quad (2.21)$$

Finally we combine equation (2.16) and (2.21) to prove the Lemma. \square

We initially need to study how the first term in equation (2.14) depends on the stochastic parameters $\{\delta_i\}_{i=1}^{n-1}$.

$$(U, \phi - \pi\phi) = \sum_{i=1}^n \int_{x_{i-1}}^{x_i} U(\phi - \pi\phi) dx \quad (2.22)$$

On each element $[x_{i-1}, x_i]$ we assume $\phi \in C^2([x_{i-1}, x_i])$ and apply Lemma 2.1 with $z = \phi - \pi\phi$, $\varphi_0 = \varphi_{i-1}$, $\varphi_1 = \varphi_i$, and $h = h_i$ to get,

$$(U, \phi - \pi\phi) = \sum_{i=1}^n \int_{x_{i-1}}^{x_i} U(\phi - \pi\phi) dx \quad (2.23)$$

$$= \sum_{i=1}^n U_{i-1} \int_{x_{i-1}}^{x_i} \varphi_{i-1}(\phi - \pi\phi)(x) dx \quad (2.24)$$

$$\begin{aligned} &+ \sum_{i=1}^n U_i \int_{x_{i-1}}^{x_i} \varphi_i(\phi - \pi\phi)(x) dx \\ &= - \sum_{i=1}^n \frac{h_i^2}{6} \int_{x_{i-1}}^{x_i} \phi'' \varphi_{i-1} \varphi_i (U(x) + U_{i-1} + U_i) dx \end{aligned} \quad (2.25)$$

$$= - \sum_{i=1}^n h_i^3 \frac{1}{h_i} \int_{x_{i-1}}^{x_i} \frac{1}{6} \phi'' \varphi_{i-1} \varphi_i (U(x) + U_{i-1} + U_i) dx. \quad (2.26)$$

We introduce the following notation,

$$z_i(\{\delta_i\}_{i=1}^{n-1}) = -\frac{k^2}{h_i} \int_{x_{i-1}}^{x_i} \frac{1}{6} \phi'' \varphi_{i-1} \varphi_i (U(x) + U_{i-1} + U_i) dx. \quad (2.27)$$

With this notation equation (2.14) and equation (2.23) now gives

$$(e, \psi) = \sum_{i=1}^n h_i^3 z_i - (\hat{p} - 1) \int_0^\pi k^2 U \pi\phi dx. \quad (2.28)$$

We now make the following simplification. We replace z_i in equation (2.28) with \bar{z}_i which is z_i calculated on a structured grid i.e.

$$\bar{z}_i = -\frac{k^2}{h} \int_{(i-1)h}^{ih} \frac{1}{6} \phi'' \bar{\varphi}_{i-1} \bar{\varphi}_i (\bar{U}(x) + \bar{U}_{i-1} + \bar{U}_i) dx, \quad (2.29)$$

where $\bar{\varphi}_i$ are the base functions on the structured grid and \bar{U} is the solution on the structured grid. This means that \bar{z}_i are not stochastic variables. We also introduce $\bar{w} = \int_0^\pi k^2 \bar{\pi} \phi(x) \bar{U}(x) dx$, where $\bar{\pi}$ is the Scott-Zhang interpolant, see [3], onto the structured grid, i.e \bar{w} is not stochastic.

If hk is small these approximations can be motivated by linearization in terms of δ but the most important argument is the good agreement we get with numerical experiments, see section 3. We define an approximation to (e, ψ) in the following way,

$$\bar{e}_\psi = \sum_{i=1}^n h_i^3 \bar{z}_i - (\hat{p} - 1) \bar{w}, \quad (2.30)$$

and we choose \hat{p} such that $\bar{e}_\psi = 0$ i.e.

$$\hat{p} = 1 + \frac{1}{\bar{w}} \sum_{i=1}^n h_i^3 \bar{z}_i. \quad (2.31)$$

Since we want to find one parameter p that suits many meshes with a given δ we study the expected value of \hat{p} . To do this we need to do the following observation,

$$E[\hat{p}] = 1 + \frac{1}{\bar{w}} E \left[\sum_{i=1}^n h_i^3 \bar{z}_i \right] \quad (2.32)$$

$$= 1 + \frac{1}{\bar{w}} \sum_{i=1}^n E[h_i^3] \bar{z}_i \quad (2.33)$$

$$= 1 + \frac{1}{\bar{w}} \sum_{i=1}^n E[(h + \delta_i - \delta_{i-1})^3] \bar{z}_i \quad (2.34)$$

$$= 1 + \frac{1}{\bar{w}} \sum_{i=1}^n E[h^3 + 3h^2(\delta_i - \delta_{i-1}) + 3h(\delta_i - \delta_{i-1})^2 + (\delta_i - \delta_{i-1})^3] \bar{z}_i \quad (2.35)$$

$$= 1 + \frac{1}{\bar{w}} \sum_{i=1}^n (h^3 + 3h^2 E[\delta_i - \delta_{i-1}]) \bar{z}_i \quad (2.36)$$

$$+ \frac{1}{\bar{w}} \sum_{i=1}^n (3h E[(\delta_i - \delta_{i-1})^2] + E[(\delta_i - \delta_{i-1})^3]) \bar{z}_i$$

$$= 1 + \frac{1}{\bar{w}} \sum_{i=1}^n (h^3 + 3h E[(\delta_i - \delta_{i-1})^2]) \bar{z}_i \quad (2.37)$$

$$= 1 + \frac{1}{\bar{w}} \sum_{i=1}^n (h^3 + 6h \text{Var}(\delta_i)) \bar{z}_i \quad (2.38)$$

$$= 1 + \frac{\sum_{i=1}^n h \bar{z}_i}{\bar{w}} (h^2 + 6 \text{Var}(\delta_i)), \quad (2.39)$$

where we use that $\{\delta_i\}_{i=1}^{n-1}$ are independent, $E[\delta_i] = 0$, and $E[\delta_i^2] = E[\delta_{i-1}^2] = \text{Var}(\delta_i)$. We neglect the boundary effect due to the fact that δ_0 and δ_n are not stochastic. If we let $\bar{z} = \sum_{i=1}^n h \bar{z}_i$ we have

$$\boxed{p = E[\hat{p}] = 1 + \frac{\bar{z}}{\bar{w}} (h^2 + 6 \text{Var}(\delta_i))} \quad (2.40)$$

Remark 2.3 For the uniform distribution $\text{Var}(\delta_i) = \frac{h^2 \delta^2}{12}$ i.e.

$$p = 1 + \frac{\bar{z}}{\bar{w}} h^2 \left(1 + \frac{\delta^2}{2} \right) \quad (2.41)$$

Remark 2.4 Given δ we can find p by using one for the standard methods [5, 2] for structured meshes and then add the contribution suggested in equation (2.41). For example if we want nodal exactness in the right endpoint $x = \pi$ we can use the formula from [5] for

nodal exactness on structured mesh to find \bar{z}/\bar{w} .

Given a formula (2.41) to find p we would like to estimate the error (e, ψ) in terms of h , k , and δ . We start by estimating the variance of \bar{e}_ψ .

Proposition 2.1 *It holds*

$$\text{Var}(\bar{e}_\psi) = h^6 \left(\frac{3}{2}\delta^2 + \frac{3}{4}\delta^4 + \frac{1}{28}\delta^6 \right) \sum_{i=1}^n \bar{z}_i^2 \quad (2.42)$$

Proof. We start from equation (2.30) with \hat{p} chosen according to equation (2.32). We note that $E[\bar{e}_\psi] = 0$ so $\text{Var}(\bar{e}_\psi) = E[\bar{e}_\psi^2]$,

$$\text{Var}(\bar{e}_\psi) = E[\bar{e}_\psi^2] \quad (2.43)$$

$$= E \left[\left(\sum_{i=1}^n h_i^3 \bar{z}_i - (\hat{p} - 1)\bar{w} \right)^2 \right] \quad (2.44)$$

$$= E \left[\left(\sum_{i=1}^n h_i^3 \bar{z}_i \right)^2 \right] - 2E \left[\sum_{i=1}^n h_i^3 \bar{z}_i \right] E[(\hat{p} - 1)\bar{w}] + E[(\hat{p} - 1)\bar{w}]^2 \quad (2.45)$$

$$= E \left[\left(\sum_{i=1}^n h_i^3 \bar{z}_i \right)^2 \right] - 2E \left[\sum_{i=1}^n h_i^3 \bar{z}_i \right] E \left[\sum_{i=1}^n h_i^3 \bar{z}_i \right] + E \left[\sum_{i=1}^n h_i^3 \bar{z}_i \right]^2 \quad (2.46)$$

$$= E \left[\left(\sum_{i=1}^n h_i^3 \bar{z}_i \right)^2 \right] - E \left[\sum_{i=1}^n h_i^3 \bar{z}_i \right]^2 \quad (2.47)$$

$$= \sum_{i=1}^n (E[h_i^6] - E[h_i^3]^2) \bar{z}_i^2. \quad (2.48)$$

We need to calculate the expected value of different powers of δ_i . We have $E[\delta_i^{2n-1}] = 0$ and

$$E[\delta_i^{2n}] = \frac{\delta^{2n} h^{2n}}{(2n+1)2^{2n}}, \quad (2.49)$$

for all $n \in \mathbf{N}$. We use these result and $h_i = h + \delta_i - \delta_{i-1}$ to get,

$$\text{Var}(\bar{e}_\psi) = \sum_{i=1}^n (E[h_i^6] - E[h_i^3]^2) \bar{z}_i^2 \quad (2.50)$$

$$= \sum_{i=1}^n h^6 \left(1 + \frac{5}{2}\delta^2 + \delta^4 + \frac{1}{28}\delta^6 - 1 - \delta^2 - \frac{1}{4}\delta^4 \right) \bar{z}_i^2 \quad (2.51)$$

$$= \sum_{i=1}^n h^6 \left(\frac{3}{2}\delta^2 + \frac{3}{4}\delta^4 + \frac{1}{28}\delta^6 \right) \bar{z}_i^2, \quad (2.52)$$

which proves the proposition. \square

We need to estimate the sum in equation (2.42) in terms of h and k . For $\psi \in H^{-1}(\Omega)$ independent of h and k we have $|\phi| \leq C/k$ for some constant C and thereby $|\phi''| \leq Ck$. The magnitude of the numeric solution U is independent of k so from equation (2.27) we get $|\bar{z}_i| \leq Ck^3$. This yields

$$\sum_{i=1}^n \bar{z}_i^2 \leq \sum_{i=1}^n Ck^6 \leq C \frac{k^6}{h}. \quad (2.53)$$

We are not interested in tracking the constants in the following theory, only the h , k , and δ dependence. If we neglect the δ^4 and δ^6 terms in Proposition 2.1 and use it together with equation (2.53) we get

$$\text{Var}(\bar{e}_\psi) \leq Ch^5 k^6 \delta^2. \quad (2.54)$$

Since $E[\bar{e}_\psi] = 0$ we can use the Chebyshev inequality to get a bound of $|\bar{e}_\psi|$,

$$P(|\bar{e}_\psi| > \epsilon) \leq \frac{\text{Var}(\bar{e}_\psi)}{\epsilon^2}. \quad (2.55)$$

By choosing $\epsilon = D\delta h^{5/2} k^3$ we get $P(|\bar{e}_\psi| > D\delta h^{5/2} k^3) \leq \frac{C}{D}$ hence with D large we can make this quantity arbitrarily small i.e. there exists C independent of δ , h , and k such that

$$\boxed{P(|\bar{e}_\psi| \leq C\delta h^{5/2} k^3) > 1 - \epsilon} \quad (2.56)$$

for each $\epsilon > 0$.

3 Numerical Results in One Dimension

We study pointwise error control. This is done by choosing ψ as the Dirac delta measure in a chosen node. We can actually find an analytic formula for the dual solution in this case,

$$\phi_z(x) = \frac{e^{ik(\pi-z)}}{ik e^{ik\pi}} \cos(kx) - \frac{1}{k} \sin(k(x-z)) I_{\{x>z\}}, \quad (3.1)$$

where z indicates a point mass in $x = z$. We note that $\phi_z(x) \in C^2([x_{i-1}, x_i])$ for $i = 1, \dots, n$. We proceed with a numerical simulation to verify that the iterative algorithm described in equation (2.13) converges and gives an optimal value of p . Figure 2 shows rapid convergence for the iterative algorithm towards machine precision. Here ψ is chosen as the dirac measure in $x = \pi$ i.e. $\psi = \delta_\pi$.

In Figure 3 we illustrate how well equation (2.41), where \bar{z}/\bar{w} is calculated on a structured mesh, compares to numerical experiments of the iterative a posteriori method, equation (2.13). For each δ , 5000 meshes have been evaluated, by iteration until convergence, and the stars are the mean value of these. The dashed line is the theoretical value of equation (2.41). We see quite a good agreement between numerics and theory. Remember

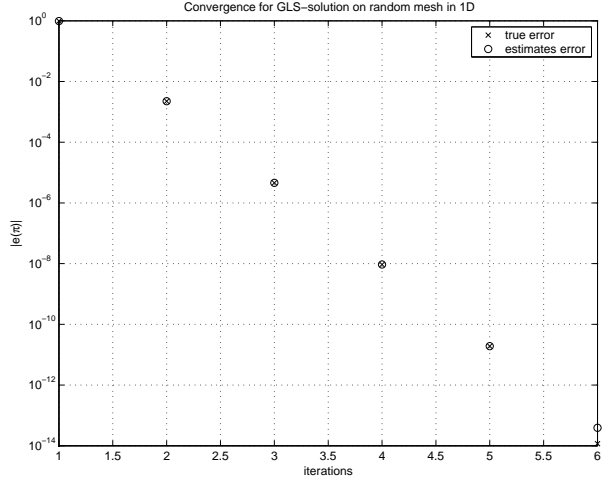


Figure 2: The error $|u(\pi) - U(\pi)|$ verses number of iterations

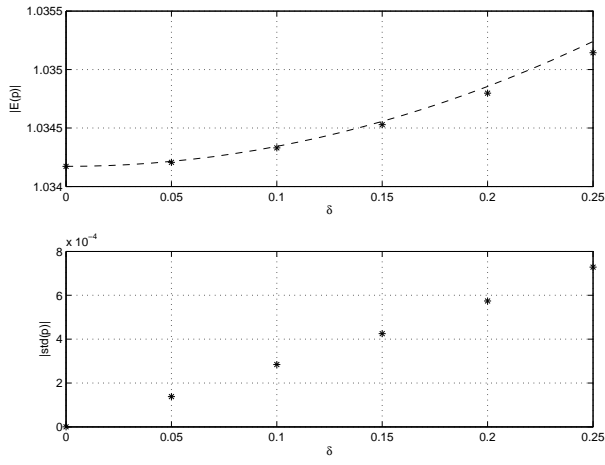


Figure 3: The expected value, $|E[\hat{p}]|$ (above), and the standard deviation, $|\sigma(\hat{p})|$ (below), verses δ .

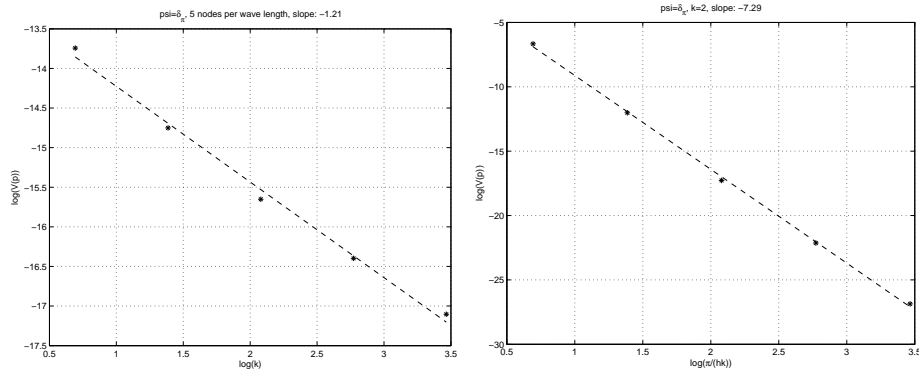


Figure 4: $\log(\text{Var}(\hat{p}))$ versus $\log k$ (left) and the logarithm of the number of nodes per wavelength (right).

that the theoretical value is based on approximations. The variance is proportional to the square of δ which agree with the theoretical result in equation (2.41).

By changing h and k separately while holding $\delta = 0.1$ we also get an idea of how the variance of \hat{p} depends on these variables, see Figure 4. In this particular case we get $\text{Var}(\hat{p}) \sim h^{7.3}k^{6.1}$ or $\text{Var}((e, \psi)) \sim h^{7.3}k^{8.1}$, since $\text{Var}((e, \psi)) \sim k^4(U, \pi\phi)^2\text{Var}(p) \sim k^2\text{Var}(p)$, which is even better than $\text{Var}(\bar{e}_\psi) \leq Ch^5k^6$ that we got from theory, see equation (2.54).

Another interesting measure of the error is the mean value i.e. $\psi = 1$. Letting $v = 1$ in (2.4) gives us, $(U, 1) = \frac{i}{kp}(1 - U(\pi))$. We have $u = e^{ikx}$ so $(u, 1) = \frac{i(1-u(\pi))}{k}$ which makes

$$(e, 1) = -\frac{i}{kp}e(\pi) + \frac{(p-1)}{p}(u, 1). \quad (3.2)$$

Since p is close to one this calculation shows that the nodal error in π is very closely related to the mean of the error and coincides if $k = 2n$, $n \in \mathbf{N}$, since $(u, 1) = 0$ in that case.

4 Two Dimensional Model Problem

In two dimensions we consider a plane wave with wave number

$$\mathbf{k} = k(\cos(\theta), \sin(\theta)) \quad (4.1)$$

propagating on a unit square, see Figure 5. We use a model problem from [5] with inhomogeneous Robin boundary conditions chosen such that the solution u is equal to $e^{i\mathbf{k}\cdot\mathbf{x}}$: find $u \in H^1(\Omega)$ such that

$$\begin{cases} -\Delta u - k^2 u = 0 & \text{in } \Omega, \\ -\partial_n u = -ik(u - g) & \text{on } \Gamma, \end{cases} \quad (4.2)$$

where Ω is a polygonal domain in \mathbf{R}^d , $d = 2, 3$ with boundary Γ .

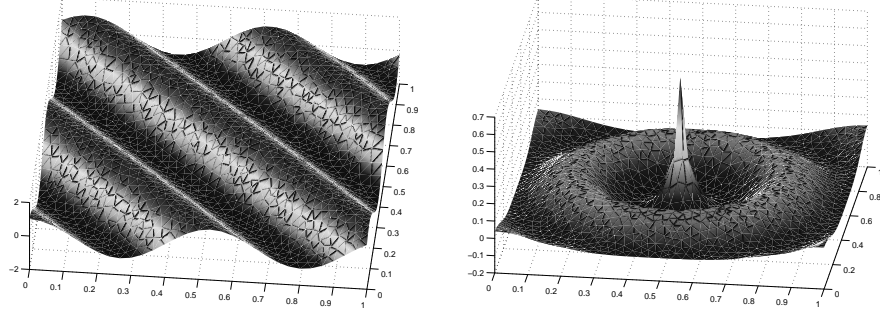


Figure 5: Real part of the solution to the primal problem with $\theta = \pi/4$ and to the dual problem with $\psi_\Omega = \delta_{[.5,.5]}$

4.1 The Galerkin Least-Squares Method

The corresponding discretized GLS method reads: find $U \in V \subset H^1(\Omega)$ such that

$$(\nabla U, \nabla v) - k^2 (U, v) + (\tau LU, Lv)_{\tilde{\Omega}} - ik(U, v)_\Gamma = -ik(g, v)_\Gamma, \quad \text{for all } v \in V, \quad (4.3)$$

where $(\cdot, \cdot)_\Gamma$ is the $L^2(\Gamma)$ scalar product, $L = -\Delta - k^2$ and V is the finite element space of piecewise polynomials of degree p . Again we want to find a criteria for choosing τ that minimizes a given linear functional of the error. We proceed as in the one dimensional case starting with the error representation formula.

4.2 Error Representation Formula

The corresponding dual problem reads: find ϕ such that

$$\begin{cases} -\Delta \phi - k^2 \phi = \psi_\Omega & \text{in } \Omega, \\ -\partial_n \phi = ik(\phi - \psi_\Gamma) & \text{on } \Gamma, \end{cases} \quad (4.4)$$

where $\psi_\Omega \in H^{-1}(\Omega)$ and $\psi_\Gamma \in H^{1/2}(\Gamma)$, see [1] for a definition of these spaces. To the right in Figure 5 we have the dual solution calculated for ψ as a point mass in $(0.5, 0.5)$. In this setting we consider two types of linear functionals of the error at the same time, namely (e, ψ_Ω) and $(e, \psi_\Gamma)_\Gamma$. The a posteriori analysis gives,

$$(e, \psi_\Omega) - ik(e, \psi_\Gamma)_\Gamma = (\nabla e, \nabla \phi) - (k^2 e, \phi) + (e, ik\phi)_\Gamma \quad (4.5)$$

$$= (\partial_n e, \phi)_\Gamma - (\nabla U, \nabla \phi) + (k^2 U, \phi) + (e, ik\phi)_\Gamma \quad (4.6)$$

$$= (ik(U - g), \phi)_\Gamma - (\nabla U, \nabla \phi - \pi \phi) + (k^2 U, \phi - \pi \phi) - (\nabla U, \nabla \pi \phi) + (k^2 U, \pi \phi) \quad (4.7)$$

$$= (\Delta U + k^2 U, \phi - \pi \phi) - (\partial_n U - ik(U - g), \phi - \pi \phi)_\Gamma + (\tau LU, L\pi \phi)_{\tilde{\Omega}}, \quad (4.8)$$

where the first scalar product in the last row is defined in the following way,

$$(\Delta U, v) = \sum_{K \in \mathcal{K}} \int_K \Delta U v dx - \sum_{K \in \mathcal{K}} \int_{\partial K \setminus \Gamma} \frac{\partial U}{\partial n_K} v ds, \quad \text{for all } v \in H^1(\Omega), \quad (4.9)$$

where K refers to elements in the mesh with boundary ∂K and $\mathcal{K} = \{K\}$ is the set of elements in the mesh. We get the following error representation formula,

$$\begin{aligned} (e, \psi_\Omega) - ik(e, \psi_\Gamma)_\Gamma &= (-LU, \phi - \pi\phi) \\ &+ (-\partial_n U + ik(U - g), \phi - \pi\phi)_\Gamma + (\tau LU, L\pi\phi)_{\tilde{\Omega}}. \end{aligned} \quad (4.10)$$

We derive a method for choosing τ by letting (4.10) be equal to zero,

$$\boxed{\tau = -\frac{(\Delta U + k^2 U, \phi - \pi\phi) - (\partial_n U - ik(U - g), \phi - \pi\phi)_\Gamma}{(LU, L\pi\phi)_{\tilde{\Omega}}}} \quad (4.11)$$

We define $(R_\Omega, v) = (\Delta U + k^2 U, v)$, for all $v \in H^1(\Omega)$, and $(R_\Gamma, v)_\Gamma = (\partial_n U + ik(U - g), v)_\Gamma$, for all $v \in H^1(\Gamma)$, as domain and boundary residual.

Again we end up with a strategy for choosing τ . As in the one-dimensional case this approach is independent of the structure of the mesh. We consider plane waves sent in different angles over the unit square. The one dimensional analysis suggests that there exists a parameter that gives us a good approximation if δ as a function of θ is close to constant. This is the case on a totally unstructured mesh but can never be the case for a structured mesh. This implies that we only need to optimize for one angle θ by the method described in equation (4.11) to get a good approximation for all angles. The reason for this is that a totally unstructured is much more isotropic than a structured mesh (if the domain is large enough).

5 Numerical Results in Two Dimensions

We study problems on two different geometries.

Example 1. First we study a plane wave on the unit square. We use the same setting as in [5] i.e. Robin type boundary conditions that approximately makes the wave propagate freely over the boundaries. Since we are interested in calculating a correction for unstructured meshes and also how this correction compares to earlier work on structured grids we start with a regular mesh constructed by the Delaunay algorithm on a two dimensional lattice. Then we add small perturbations to the interior nodes and proceed with another Delaunay triangulation, see Figure 6. We introduce a parameter $\boldsymbol{\delta}$ in analogy with the one dimensional case that measure how unstructured the mesh is. Now the perturbation of the interior nodes are done both in x and y direction so $\boldsymbol{\delta}$ has two entries (δ_x, δ_y) . Below $\delta_x = \delta_y = \delta$ if nothing else is mentioned. On these meshes we calculate an optimal p for error control on the outflow boundary Γ_o when the wave propagates in the x -direction i.e.

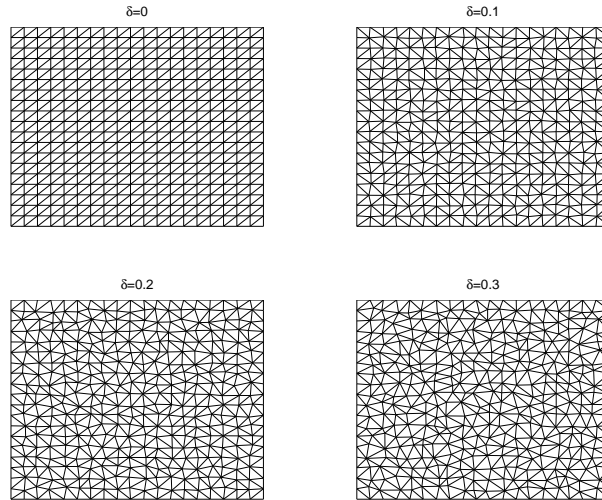


Figure 6: Delaunay triangulations with various δ .

$\theta = 0$. This means that $\Gamma_o = \{(x, y) : x = 1, 0 \leq y \leq 1\}$. In equation (4.10) this is achieved by letting $\psi_\Omega = 0$ and $\psi_\Gamma = I_{\Gamma_o}$ to get ϕ and then using equation (4.11). To get small error i.e. find the optimal p we repeat this process iteratively in analogy with equation (2.13) until the error is about one millionth of the Galerkin error.

In Figure 7 we see how p depends on δ . It is slowly increasing for small δ except a jump between $\delta = 0$ and $\delta = 0.05$ depending on the big structural change in the grid. For $\delta = 0$ we have a regular mesh and for $\delta = 0.05$ we get an approximate union jack shape. For bigger δ we see that p increases in the same way as in the one dimensional case. The dashed lines are from a classic GLS-method optimized for the regular mesh, $\delta = 0$ in Figure 6, and the standard Galerkin method, $p = 1$. In this example $k = 20$.

The similarities with the one dimensional result does not come as a surprise. Since the dual solution is independent of y in this particular example we can use equation (4.11) to

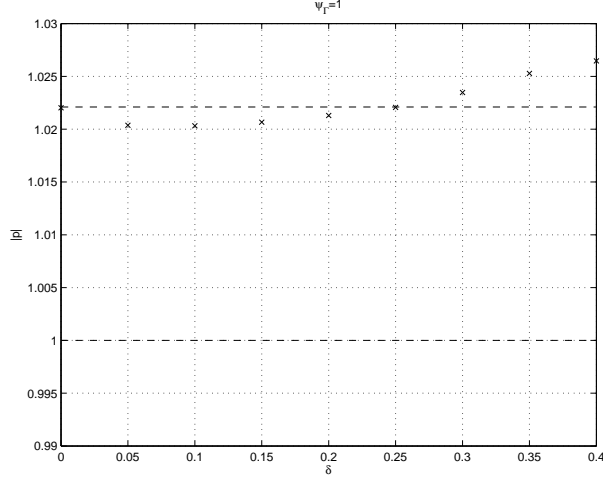


Figure 7: p optimized for error control with $\psi_\Omega = 0$ and $\psi_\Gamma = I_{\Gamma_o}$ on various unstructured meshes.

proceed with the following heuristic calculation,

$$-\tau(LU, L\pi\phi)_{\tilde{\Omega}} = (R_\Omega, \phi - \pi\phi) + (R_\Gamma, \phi - \pi\phi)_\Gamma \quad (5.1)$$

$$= \int_0^1 \int_0^1 R_\Omega(\phi - \pi\phi) dy dx \quad (5.2)$$

$$+ \int_{\{x \in [0,1], y=0\}} R_\Gamma(\phi - \pi\phi) dx$$

$$- \int_{\{x \in [0,1], y=1\}} R_\Gamma(\phi - \pi\phi) dx$$

$$\approx \int_0^1 (\phi - \pi\phi) \int_0^1 R_\Omega dy dx + \int_0^1 C(x)(\phi - \pi\phi) dx \quad (5.3)$$

$$= \int_0^1 D(x)(\phi - \pi\phi) dx. \quad (5.4)$$

Using the one dimensional result in equation (2.41) and that $(LU, L\pi\phi)_{\tilde{\Omega}}$ should not depend heavily on δ we get that $\tau \sim h^2 + C\text{Var}(\delta_x) \sim h^2(1 + C\delta_x^2)$. The additional assumption we need to do in this case is that also $\pi\phi$ is almost constant in the y direction.

We note one difference that actually suggests better results in the two dimensional case when the error is integrated over the outflow boundary. Instead of having essentially $e = \int R\phi dx$, where R is the residual, we get in two dimensions $e = \int(\int R dy)\phi dx$ i.e. an integral over the residual in the y -direction. This would decrease the variance of the error and therefore also the error bound by the Chebyshev inequality in equation (2.54).

Numerical results confirms this. We let δ and hk be constant and k to be free. The variance of $ik(e, I_{\Gamma_o})_\Gamma$ is computed for 100 different meshes in Figure 8. As seen to the

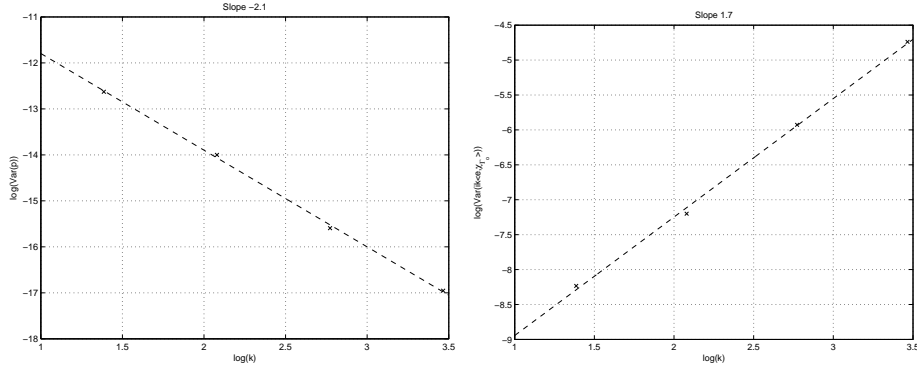


Figure 8: $\text{Var}(p)$ (left) and $\text{Var}(ik(e, I_{\Gamma_o})_{\Gamma})$ (right) dependence of k when $\delta = 0.3$ and kh is hold constant.

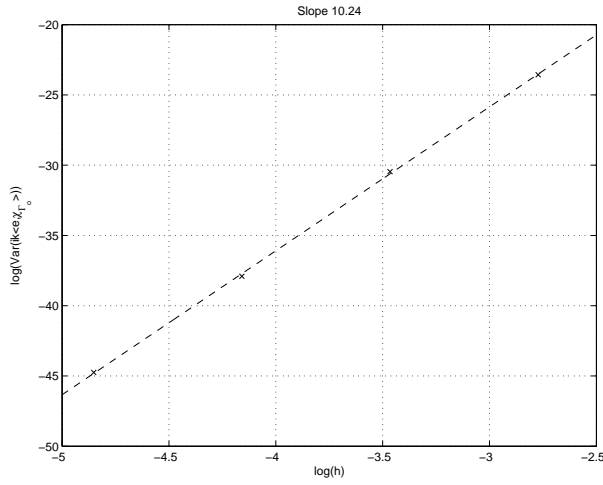


Figure 9: $\text{Var}(ik(e, I_{\Gamma_o})_{\Gamma})$ verses h with constant $k = 4$ and $\delta = 0.3$.

left in Figure 8 $\text{Var}(p) \sim (hk)^{\alpha}k^{-2}$ for some α . With a similar calculation as in the one dimensional case we get $\text{Var}(ik(e, I_{\Gamma_o})_{\Gamma}) = k^4(U, \pi\phi)^2\text{Var}(p)$ and since $(U, \pi\phi) \sim 1$ we get $\text{Var}((e, I_{\Gamma_o})_{\Gamma}) \sim k^2\text{Var}(p) \sim (hk)^{\alpha}$. We see this in the right plot in Figure 8 where we plot $\text{Var}(ik(e, I_{\Gamma_o})_{\Gamma})$ verses k while holding hk constant. To determine α we perform another test where we vary h while holding k constant. The result is presented in Figure 9. We see that α is approximately equal to 10 i.e. as we suspected we gain one h compared to the one dimensional case,

$$\text{Var}((e, I_{\Gamma_o})_{\Gamma}) \sim (hk)^{10}, \quad (5.5)$$

and from the Chebyshev inequality we get from these numerical tests

$$\boxed{P(|(e, I_{\Gamma_o})_{\Gamma}| \leq C(hk)^5) \geq 1 - \epsilon} \quad (5.6)$$

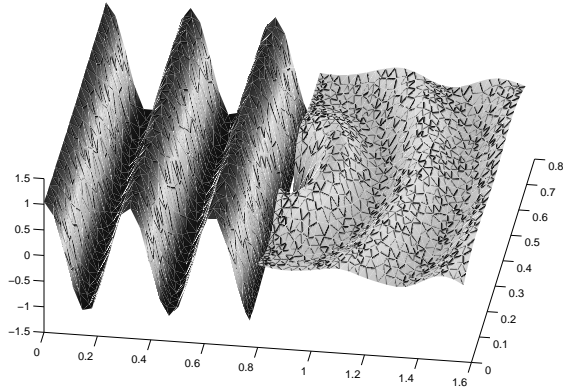


Figure 10: Real part of the solution using our method to determine τ . $\epsilon_x = 0.03$ and $\epsilon_y = 0.1$.

for $\epsilon > 0$ i.e. we have no pollution effect for error control in this specific norm on meshes with constant δ .

The variance of the error can also measure the angle depends in the method. With this result we would not expect worse angle dependence when k increases and hk is hold constant which is a very nice result.

Example 2. Finally we consider a bit more complicated problem where we simulate waves travelling through a slit of width ϵ_y and thickness ϵ_x . The domain is a rectangle of length $\pi/2$ and hight $\pi/4$ with two ϵ_x wide walls in the middle only leaving a gap of ϵ_y between them. The wave number is set to 20 so we expect five full waves in the centre of the domain $y = \pi/8$. The real part of the solution of the primal and dual are presented in Figure 10 and Figure 11. The dual solution is calculated for nodal error control in $(x, y) = (\pi/2, \pi/8)$. The wave plane propagates towards the slit and creates approximately a point source at the slit. We get the characteristic circular waves as when rocks falls into the sea continuously in one point. The amplitude decreases as the wave propagates away from the slit in the same way as the dual solution decays from the point mass in $(x, y) = (\pi/2, \pi/8)$.

6 Conclusion

We have discussed how and when standard methods for solving the pollution problem on structured grids needs to be modified to suit unstructured grids. The analysis is based on a posteriori error estimates of model problems in one and two dimensions. We present numerical simulations that confirms our theoretical results on both one and two dimensions.

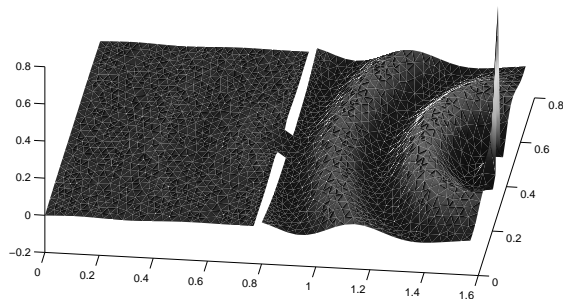


Figure 11: Real part of the dual solution for error control in $(x, y) = (\pi/2, \pi/8)$.

References

- [1] R. A. Adams, *Sobolev spaces*, volume 65 of Pure and Applied Mathematics, Academic Press, New York, 1975.
- [2] I. Babuška, F. Ihlenburg, E. T. Paik and S. A. Sauter, *A generalised finite element method for solving the Helmholtz equation in two dimensions with minimal pollution*, *Comput. Methods Appl. Mech. Engrg.*, 128(1995), 325-359.
- [3] S. C. Brenner and L. R. Scott, *The mathematical theory of finite element methods*, Springer Verlag, 1994.
- [4] K. Eriksson, D. Estep, P. Hansbo and C. Johnson, *Computational differential equations*, Studentlitteratur, 1996.
- [5] I. Harari and C. L. Nogueira, *Reducing dispersion of linear triangular elements for the Helmholtz equation*, *J. of Eng. Mech.*, 128(3), 351-358, 2002.
- [6] I. Harari and T. J.R. Hughes, *Galerkin/least-squares finite element methods for the reduced wave equation with non-reflecting boundary conditions in unbounded domains*, *Comput. Methods Appl. Mech. and Engrg.*, 98(1992), 411-454.
- [7] T. J.R. Hughes, G. R. Feijóo, L. Mazzei, J.-B. Quincy, *The variational multiscale method - a paradigm for computational mechanics*, *Comput. Methods Appl. Mech. and Engrg.*, 166(1998), 3-24.
- [8] A. A. Oberai and P. M. Pinsky, *A multiscale finite element method for the Helmholtz equation*, *Comput. Methods Appl. Mech. Engrg.* 154, 281-297, 1998.

- [9] A. A. Oberai and P. M. Pinsky, *A residual-based finite element method for the Helmholtz equation*, Int. J. Numer. Meth. Engng. 49(2000):399-419.
- [10] J.-Y. Wu and R. Lee, *The advantages of triangular and tetrahedral edge elements for electro magnetic modelling with the finite-element method*, IEEE trans. Antennas Propagat., 45(9), 1997.

Chalmers Finite Element Center Preprints

- 2003–01** *A hybrid method for elastic waves*
L.Beilina
- 2003–02** *Application of the local nonobtuse tetrahedral refinement techniques near Fichera-like corners*
L.Beilina, S.Korotov and M. Křížek
- 2003–03** *Nitsche’s method for coupling non-matching meshes in fluid-structure vibration problems*
Peter Hansbo and Joakim Hermansson
- 2003–04** *Crouzeix–Raviart and Raviart–Thomas elements for acoustic fluid–structure interaction*
Joakim Hermansson
- 2003–05** *Smoothing properties and approximation of time derivatives in multistep backward difference methods for linear parabolic equations*
Yubin Yan
- 2003–06** *Postprocessing the finite element method for semilinear parabolic problems*
Yubin Yan
- 2003–07** *The finite element method for a linear stochastic parabolic partial differential equation driven by additive noise*
Yubin Yan
- 2003–08** *A finite element method for a nonlinear stochastic parabolic equation*
Yubin Yan
- 2003–09** *A finite element method for the simulation of strong and weak discontinuities in elasticity*
Anita Hansbo and Peter Hansbo
- 2003–10** *Generalized Green’s functions and the effective domain of influence*
Donald Estep, Michael Holst, and Mats G. Larson
- 2003–11** *Adaptive finite element/difference method for inverse elastic scattering waves*
L.Beilina
- 2003–12** *A Lagrange multiplier method for the finite element solution of elliptic domain decomposition problems using non-matching meshes*
Peter Hansbo, Carlo Lovadina, Ilaria Perugia, and Giancarlo Sangalli
- 2003–13** *A reduced P^1 –discontinuous Galerkin method*
R. Becker, E. Burman, P. Hansbo, and M. G. Larson
- 2003–14** *Nitsche’s method combined with space–time finite elements for ALE fluid–structure interaction problems*
Peter Hansbo, Joakim Hermansson, and Thomas Svedberg
- 2003–15** *Stabilized Crouzeix–Raviart element for the Darcy–Stokes problem*
Erik Burman and Peter Hansbo

- 2003–16** *Edge stabilization for the generalized Stokes problem: a continuous interior penalty method*
Erik Burman and Peter Hansbo
- 2003–17** *A conservative flux for the continuous Galerkin method based on discontinuous enrichment*
Mats G. Larson and A. Jonas Niklasson
- 2003–18** *CAD-to-CAE integration through automated model simplification and adaptive modelling*
K.Y. Lee, M.A. Price, C.G. Armstrong, M.G. Larson, and K. Samuelsson
- 2003–19** *Multi-adaptive time integration*
Anders Logg
- 2003–20** *Adaptive computational methods for parabolic problems*
Kenneth Eriksson, Claes Johnson, and Anders Logg
- 2003–21** *The FEniCS project*
T. Dupont, J. Hoffman, C. Johnson, R. Kirby, M. Larson, A. Logg, and R. Scott
- 2003–22** *Adaptive finite element methods for LES: Computation of the mean drag coefficient in a turbulent flow around a surface mounted cube using adaptive mesh refinement*
Johan Hoffman
- 2003–23** *Adaptive DNS/LES: a new agenda in CFD*
Johan Hoffman and Claes Johnson
- 2003–24** *Multiscale convergence and reiterated homogenization of parabolic problem*
Anders Holmbom, Nils Svanstedt, and Niklas Wellander
- 2003–25** *On the relationship between some weak compactnesses with different numbers of scales*
Anders Holmbom, Jeanette Silfver, Nils Svanstedt, and Niklas Wellander
- 2003–26** *A posteriori error estimation in computational inverse scattering*
Larisa Beilina and Claes Johnson
- 2004–01** *Computability and adaptivity in CFD*
Johan Hoffman och Claes Johnson
- 2004–02** *Interpolation estimates for piecewise smooth functions in one dimension*
Anders Logg
- 2004–03** *Estimates of derivatives and jumps across element boundaries for multi-adaptive Galerkin solutions of ODEs*
Anders Logg
- 2004–04** *Multi-adaptive Galerkin methods for ODEs III: Existence and stability*
Anders Logg
- 2004–05** *Multi-adaptive Galerkin methods for ODEs IV: A priori error estimates*
Anders Logg
- 2004–06** *A stabilized non-conforming finite element method for incompressible flow*
Erik Burman and Peter Hansbo
- 2004–07** *On the uniqueness of weak solutions of Navier-Stokes equations: Remarks on a Clay Institute prize problem*
Johan Hoffman and Claes Johnson

- 2004–08** *A new approach to computational turbulence modeling*
Johan Hoffman and Claes Johnson
- 2004–09** *A posteriori error analysis of the boundary penalty method*
Kenneth Eriksson, Mats G. Larson, and Axel Målqvist
- 2004–10** *A posteriori error analysis of stabilized finite element approximations of the
helmholtz equation on unstructured grids*
Mats G. Larson and Axel Målqvist

These preprints can be obtained from

www.phi.chalmers.se/preprints